

Estimated PDFs of climate system properties including natural and anthropogenic forcings

Chris E. Forest, Peter H. Stone, and Andrei P. Sokolov

Joint Program on the Science and Policy of Global Change, Department of Earth, Atmospheric and Planetary Sciences, Massachusetts Institute of Technology, Cambridge, Massachusetts, USA

Received 20 July 2005; revised 30 November 2005; accepted 2 December 2005; published 13 January 2006.

[1] We present revised probability density functions (PDF) for climate system properties (climate sensitivity, rate of deep-ocean heat uptake, and the net aerosol forcing strength) that include the effect on 20th century temperature changes of natural as well as anthropogenic forcings. The additional natural forcings, primarily the cooling by volcanic eruptions, affect the PDF by requiring a higher climate sensitivity and a lower rate of deep-ocean heat uptake to reproduce the observed temperature changes. The estimated 90% range of climate sensitivity is 2.1 to 8.9 K. The net aerosol forcing strength for the 1980s shifted toward positive values to compensate for the volcanic forcing with 90% bounds of -0.74 to -0.14 W/m². The rate of deep-ocean heat uptake is reduced with the effective diffusivity, K_v , ranging from 0.05 to 4.1 cm²/s. This upper bound implies that many AOGCMs mix heat into the deep ocean (below the mixed layer) too efficiently. **Citation:** Forest, C. E., P. H. Stone, and A. P. Sokolov (2006), Estimated PDFs of climate system properties including natural and anthropogenic forcings, *Geophys. Res. Lett.*, 33, L01705, doi:10.1029/2005GL023977.

1. Introduction

[2] *Forest et al.* [2002] presented an estimate of the joint probability density function (PDF) for uncertain climate system properties. Other groups [*Andronova and Schlesinger*, 2001; *Gregory et al.*, 2002; *Knutti et al.*, 2003] have estimated similar PDFs although each uses different methods and data. However all are based on estimating the degree to which a climate model can reproduce the historical climate record. Parameters within each model are perturbed to alter the response to climate forcings and a statistical comparison is used to reject combinations of model parameters.

[3] We use an optimal fingerprint detection technique for comparing model and observational data. This technique consists of running a climate model under a set of prescribed forcings and using climate change detection diagnostics to determine whether the simulated climate change is observed in the climate record and is distinguishable from unforced variability of the climate system (see *Mitchell et al.* [2001] or *International ad hoc Detection and Attribution Group* [2005] and references therein). It is not possible to estimate the true climate system variability on century time-scales from observations and therefore, climate models are run with fixed boundary conditions for thousands of years to obtain estimates of the climate variability.

[4] *Forest et al.* [2001, 2002] developed a method to analyze uncertainty in climate sensitivity (S), the rate of heat uptake by the deep ocean (K_v), and the net aerosol forcing (F_{aer}). These factors ($\theta = S, K_v, F_{\text{aer}}$) were constrained by using three different diagnostics to estimate the probability of rejection for combinations of model parameters that lead to simulations of the 20th century which are inconsistent with the observed records of climate change. The PDFs from each diagnostic can be combined to provide stronger constraints for the uncertain properties via an application of Bayes' Theorem. A simplified model is required because the most sophisticated models are computationally too inefficient.

[5] Two significant additions are presented here. First, our former analysis only considered effects from anthropogenic forcings (discussed later) while now we also account for two natural forcings and one additional anthropogenic one. In our earlier study, the sulfate aerosol pattern had a specified dependence on latitude and surface type, but the amplitude was taken to be one of the uncertain parameters to be constrained. Although additional uncertainties are associated with the newly added forcings, they are generally believed to be smaller than the uncertainties associated with sulfate aerosols [*Hansen et al.*, 2002]. Thus, in our new analysis, we retain the amplitude of the sulfate aerosol forcing as the only uncertain parameter describing the forcing. However, we do include in this paper some tests of whether our new results are sensitive to uncertainties in the new forcings.

2. Methodology

[6] To quantify uncertainty in climate model properties, the basic method [*Forest et al.*, 2001, 2002] can be summarized as consisting of two parts: simulations of the 20th century climate record and the comparison of the simulations with observations using optimal fingerprint diagnostics. First, we require a large sample of simulated records of climate change in which climate parameters have been systematically varied. This requires a computationally efficient model with variable parameters as provided by the MIT 2D statistical-dynamical climate model [*Sokolov and Stone*, 1998]. A brief description of the MIT 2D climate model and its recent modifications are given in the auxiliary material¹. Second, we employ a method of comparing model data to observations that appropriately filters "noise" from the pattern of climate change. The variant of optimal fingerprinting proposed by *Allen and Tett* [1999] provides

this tool and yields detection diagnostics that are objective estimates of model-data goodness-of-fit. These goodness of fit statistics are then used to estimate the likely value of uncertain parameters (via a likelihood function, $L(\theta)$) for each diagnostic of climate change. Individual $L(\theta)$ are then combined to estimate the posterior distribution, $p(\theta|\Delta T_i, C_N)$, where ΔT_i represent the three temperature change patterns and C_N is the noise covariance matrix required to estimate the goodness-of-fit statistics. The three diagnostics remain unchanged (see the auxiliary material) although the deep-ocean temperature data from *Levitus et al.* [2000] have been replaced with *Levitus et al.* [2005]. The interdecadal variability of these data have been questioned [Gregory et al., 2004], however, we partially avoid this problem by using the linear trend as our diagnostic and including the analysis error estimates from *Levitus et al.* [2005] in the noise estimate. The observation periods are 1906–1995 (surface), 1961–1995 (upper-air), and 1955–1995 (deep-ocean).

[7] In this work, the noise covariance matrix has been estimated from multiple control runs of AOGCMs. The matrix represents the natural variability in any predicted pattern which is determined by the variability in the corresponding pattern amplitude in successive segments of “pseudo-observations” extracted from the control run for the climate model. The variability of the MIT 2D climate model is somewhat lower than that of AOGCMs [Sokolov and Stone, 1998], but the model does exhibit changes in variability which are dependent on S and K_v and are similar to results from *Wigley and Raper* [1990].

3. Experimental Design

[8] The description of the climate model experiments, the ensemble design, and the algorithm for estimating the joint PDFs are given by *Forest et al.* [2001, 2002]. The major change in the new experiments is the inclusion of three additional 20th century forcings during the period 1860–1995. The set of forcings is now greenhouse gas concentrations, sulfate aerosol loadings, tropospheric and stratospheric ozone concentrations, land-use vegetation changes [Ramankutty and Foley, 1999], solar irradiance changes [Lean, 2000], and stratospheric aerosols from volcanic eruptions [Sato et al., 1993]. We refer to these forcings as GSOLSV with the first three, GSO, being those used by *Forest et al.* [2002]. (Details on all forcings are in the auxiliary material.)

[9] Additionally, we elected to run each perturbation of the 4 member ensemble starting with different initial conditions in 1860 rather than perturbing the climate system in 1940 as done previously. This provides data for each ensemble member for the entire simulation as we use surface temperatures beginning in 1906. The initial conditions for each ensemble member were taken every ten years from an equilibrium control simulation. In total, 271,456 simulation years were required.

4. Results

[10] In the simulated climate change, the additional forcings have two major effects that can be illustrated by examining the simulated response to the GSOLSV and GSO forcings and comparing with the observed records,

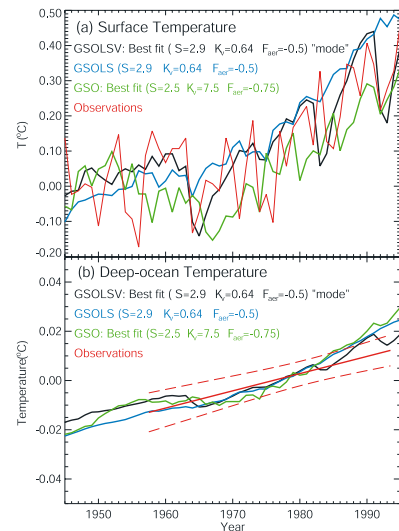


Figure 1. Representative MIT 2D model simulations with the GSOLSV, GSOLS, and GSO forcings for global-mean annual-mean surface temperature change (a) and 0–3 km global-mean annual-mean ocean temperature change (b). We show cases near the distributions’ modes for GSOLSV (black) and GSOLS (cyan) and for GSO (green). Observations (red) from P. D. Jones (<http://www.cru.uea.ac.uk/cru/data/temperature/>, 2000) (surface) and the estimated trend and its uncertainty from *Levitus et al.* [2005] (deep-ocean). Anomaly reference periods: 1906–1995 (Figure 1a), 1955–1995 (Figure 1b).

directly (Figure 1). The new results indicate higher S , lower K_v , and slightly weaker F_{aer} . These shifts in the distributions are summarized as follows. The inclusion of the volcanic aerosol forcing provides a net surface cooling during the latter 20th century (Figure 1). This requires changes in uncertain model parameters to remain consistent with the historical climate record (Figures 2 and 3) which can be achieved by reducing K_v or F_{aer} , increasing S , or combinations of all three. The mode for F_{aer} is partially reduced from -0.7 to -0.5 W/m^2 but there is little change in the distribution’s width with the 5–95 percentile range being 0.6 W/m^2 . The reduction in the mode is partially because F_{aer} no longer includes the volcanic term. However, the net aerosol forcing remains a cooling effect. The modes for S , K_v , and F_{aer} are 2.9 K, 0.65 cm^2/s , and -0.5 W/m^2 , respectively, for the distributions using uniform priors.

[11] The new distributions are compared with those of *Forest et al.* [2002] in Figure 2, and two key comparisons are made. In one, we compare the distributions with identical treatments of the climate change diagnostics by keeping the number of retained EOFs (κ) in the decomposition of $C_N^{-1}(\kappa)$ fixed. Thus, for the surface temperature diagnostic, we use $\kappa_{\text{sfc}} = 14$ in both the GSO and GSOLSV PDFs and the marginal posterior distributions for S , F_{aer} , and K_v are altered. In the second comparison, we vary κ_{sfc} . For the surface data, *Forest et al.* [2002] found that we could reject $\kappa_{\text{sfc}} > 14$ based on the *Allen and Tett* [1999] criterion. With the additional forcings, we are no longer able to reject the higher EOFs and find that the distributions are insensitive for $15 < \kappa_{\text{sfc}} < 19$. In a separate work on Bayesian selection criteria, *Curry et al.* [2005] using our

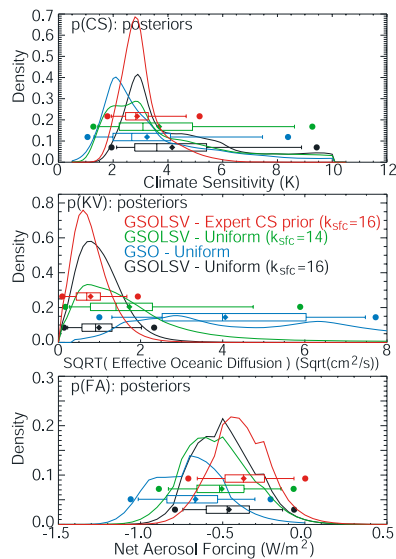


Figure 2. Marginal posterior PDF for the three climate system properties for four cases. In each panel, the marginal PDFs are shown for the GSOLSV forcings with $\kappa_{\text{sfc}} = 16$ (black) and 14 (green) and for GSO case (blue) with $\kappa_{\text{sfc}} = 14$ from *Forest et al.* [2002]. A fourth case (red) includes an expert prior on S and uniform priors elsewhere with $\kappa_{\text{sfc}} = 16$. The whisker plots indicate boundaries for the percentiles 2.5–97.5 (dots), 5–95 (vertical bar at ends), 25–75 (box ends), and 50 (vertical bar in box). The mean is indicated with the diamond and the mode is the peak in the distribution. The range for S is 0.5–10 K while ranges for K_v and F_{aer} are given by plot boundaries.

data find that a break occurs at $\kappa_{\text{sfc}} = 16$ and thus we select this as an appropriate cutoff. This inclusion of higher order EOFs is equivalent to stating that smaller spatial and temporal scale patterns (in five decadal means and four equal-area zonal averages) present in the GSOLSV response are consistent with similar patterns in the observations, unlike the GSO case. As a final issue, this shift from $\kappa_{\text{sfc}} = 14$ to 15 further limits the higher K_v values. We note that the range of effective ocean diffusivities for the existing AOGCMs is 4–25 cm^2/s [*Sokolov et al.*, 2003], and these values appear to be highly unlikely according to our new results. We note that the deep ocean temperatures used here have a 20% weaker trend than those used in our previous analysis, and this is one reason why the acceptable values of K_v are now lower. However, the upper bound on K_v results from the combination of the surface and deep-ocean temperature diagnostics (depending on the region of the parameter space (see the auxiliary material)).

[12] Several sensitivity tests were performed to assess the robustness of the estimated distributions. Specifics are given in the auxiliary material, but we briefly discuss two here. A first test determines whether the location of the deep-ocean heat uptake influenced the spatio-temporal patterns of temperature change. The latitude dependence of K_v , which was based on observations of tritium mixing [*Sokolov and Stone*, 1998], was changed to reflect the pattern identified in the ocean data [*Levitus et al.*, 2000]. Although local surface temperatures were changed, the large-scale averages (four equal-area zonal bands) used in our diagnostics were not

affected. A second test explored the sensitivity of the results to reducing the strength of the volcanic forcing by 25%. This requires stronger F_{aer} cooling and lower S values to bring the temperature response down to match the observations but the changes are relatively small. These results suggest that the PDFs are robust to such changes.

[13] Since the estimated distributions depend on the truncation for the eigendecomposition of C_N for the surface temperature diagnostic, we tested the impact of uncertainty in C_N by using estimates based on the natural variability from control runs by the HadCM2, HadCM3, GFDL_R30, and PCM models. The resulting PDFs did not differ qualitatively (results not shown). Although the results are not sensitive to the choice of AOGCM, observations do not exist to test the quality of such estimates.

5. Discussion and Conclusions

[14] We present revised PDFs for climate system properties that now include the response to both natural and anthropogenic forcings. With additional new forcings, a larger climate sensitivity and a reduced rate of ocean heat uptake below the mixed layer are required to match the observed climate record in the 20th century. The primary factor leading to this change is the strong cooling forcing by volcanic eruptions through the stratospheric aerosols. Similarly, there is a small change in the aerosol forcing which tends to offset the volcanic cooling. When using uniform priors on all parameters, these new results are summarized by the 90% confidence bounds of 2.1 to 8.9 K for climate sensitivity, 0.05 to 4.1 cm^2/s for K_v , and -0.74 to -0.14 W/m^2 for the net aerosol forcing strength. We note that the upper bound for the climate sensitivity is sensitive to our choice of prior, which was truncated at 10 K. When an expert prior for S is used [*Forest et al.*, 2002], the 90% confidence

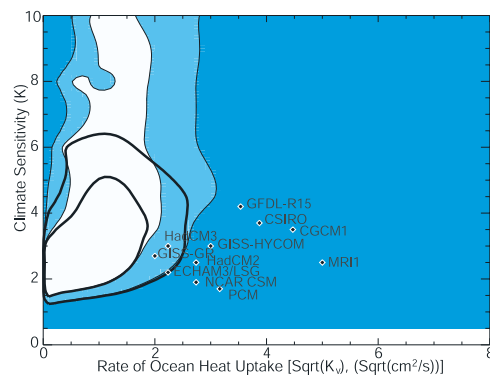


Figure 3. Marginal posterior PDF for GSOLSV results with uniform priors for the S - K_v parameter space. The shading denotes rejection regions for the 10%, and 1% significance levels, light to dark, respectively. The 10%, and 1% boundaries for the posterior with expert prior on S are shown by thick black contours. The positions of AOGCMs [from *Sokolov et al.*, 2003] represent the parameter values required in the MIT 2D model to match the transient response in surface temperature and thermal expansion component of sea-level rise. Lower K_v values imply less deep-ocean heat uptake and hence, a smaller effective heat capacity of the ocean.

intervals are 1.9 to 4.7 K, 0.02 to 2.9 cm²/s, and -0.65 to -0.07 W/m² for S , K_v , and F_{aer} , respectively. We note that our PDF for S has a similar shape to PDFs in other studies [e.g., Knutti et al., 2003], although our results differ significantly in having a higher lower bound on S .

[15] Our new estimates for K_v imply that most AOGCMs are mixing heat into the deep ocean too efficiently, as shown in Figure 3. We stress that K_v represents the rate of deep-ocean heat uptake and note that the net temperature change (surface or deep-ocean) will be defined by multiple factors including S and F_{aer} . A number of studies (see a detailed discussion and references in the auxiliary material) have reported the detection of the anthropogenic signal in the Levitus et al. [2000, 2005] ocean temperature data; however, one can obtain a correct temperature change with excessive mixing if S is too low, for example. Hence a single diagnostic is not sufficient to describe fully the model response.

[16] From the two sensitivity tests regarding the strength of the volcanic forcing and the location of the ocean heat uptake, we find that our results appear robust. We note that uncertainties in the volcanic forcing will alter the posterior distribution and could increase S if it were larger. We also explored the sensitivity to the estimated $C_N^{-1}(\kappa)$ and found that although the specific AOGCM is not very important, the method for truncating the number of retained eigenvectors (i.e., patterns of unforced variability) is critical. Based on $\kappa_{\text{sfc}} = 14, 15, \text{ or } 20$, the robust result is that the lower bound on S is higher and failure to reject $S > 5$ K remains. Additionally, for all three choices, high K_v values are rejected as producing too much ocean heat uptake and the net aerosol forcing uncertainty remains stable. The best choice appears to be $\kappa_{\text{sfc}} = 16$.

[17] Finally, the use of the expert prior on S remains a key factor in limiting the possibility of high values of S . Despite their uncertainties, the paleoclimate results provide data not directly included in the present framework [Hansen et al., 1993] and this supports using a prior influenced by such results. The implications of these results are that the climate system response will be stronger (specifically, a higher lower bound) for a given forcing scenario than previously estimated via the uncertainty propagation techniques of Webster et al. [2003].

[18] **Acknowledgments.** We thank many scientists who have encouraged this work including Myles Allen (Oxford) and Jim Hansen (MIT), the support of the Joint Program on the Science and Policy of Global Change at MIT, and two anonymous reviewers for helpful comments. This work was supported in part by the NOAA Office of Global Programs and by the Office of Science (BER), U.S. Department of Energy, grant DE-FG02-93ER61677. The views, opinions, and findings contained in this report are those of the authors.

References

- Allen, M. R., and S. F. B. Tett (1999), Checking for model consistency in optimal fingerprinting, *Clim. Dyn.*, *15*, 419–434.
- Andronova, N. G., and M. E. Schlesinger (2001), Objective estimation of the probability density function for climate sensitivity, *J. Geophys. Res.*, *106*(D19), 22,605–22,612.
- Curry, C. T., B. Sanso, and C. E. Forest (2005), Inference for climate system properties, *AMS Tech. Rep. ams2005-13*, Am. Stat. Assoc., Alexandria, Va.
- Forest, C. E., M. R. Allen, A. P. Sokolov, and P. H. Stone (2001), Constraining climate model properties using optimal fingerprint detection methods, *Clim. Dyn.*, *18*, 277–295.
- Forest, C. E., P. H. Stone, A. P. Sokolov, M. R. Allen, and M. D. Webster (2002), Quantifying uncertainties in climate system properties with the use of recent climate observations., *Science*, *295*, 113–117.
- Gregory, J., R. Stouffer, S. Raper, P. Stott, and N. Rayner (2002), An observationally based estimate of the climate sensitivity, *J. Clim.*, *15*, 3117–3121.
- Gregory, J. M., H. T. Banks, P. A. Stott, J. A. Lowe, and M. D. Palmer (2004), Simulated and observed decadal variability in ocean heat content, *Geophys. Res. Lett.*, *31*, L15312, doi:10.1029/2004GL020258.
- Hansen, J., A. Lacis, R. Ruedy, M. Sato, and H. Wilson (1993), How sensitive is the world's climate?, *Natl. Geogr. Res. Explor.*, *9*, 142–158.
- Hansen, J., et al. (2002), Climate forcings in Goddard Institute for Space Studies S12000 simulations, *J. Geophys. Res.*, *107*(D18), 4347, doi:10.1029/2001JD001143.
- International ad hoc Detection and Attribution Group (2005), Detecting and attributing external influences on the climate system: A review of recent advances, *J. Clim.*, *18*, 1291–1314.
- Knutti, R., T. F. Stocker, F. Joos, and G. Plattner (2003), Probabilistic climate change projections using neural networks, *Clim. Dyn.*, *21*, 257–272.
- Lean, J. (2000), Evolution of the sun's spectral irradiance since the maunder minimum, *Geophys. Res. Lett.*, *27*, 2421–2424.
- Levitus, S., J. Antonov, T. P. Boyer, and C. Stephens (2000), Warming of the world ocean, *Science*, *287*, 2225–2229.
- Levitus, S., J. Antonov, and T. Boyer (2005), Warming of the world ocean, 1955–2003, *Geophys. Res. Lett.*, *32*, L02604, doi:10.1029/2004GL021592.
- Mitchell, J. F. B., et al. (2001), Detection of climate change and attribution of causes, in *Climate Change 2001: The Scientific Basis*, edited by J. T. Houghton et al., pp. 695–738, Cambridge Univ. Press, New York.
- Ramankutty, N., and J. A. Foley (1999), Estimating historical changes in global land cover: Croplands from 1700 to 1992, *Global Biogeochem. Cycles*, *13*(4), 997–1027.
- Sato, M., J. E. Hansen, M. P. McCormick, and J. B. Pollack (1993), Stratospheric aerosol optical depths, *J. Geophys. Res.*, *98*, 22,987–22,994.
- Sokolov, A. P., and P. H. Stone (1998), A flexible climate model for use in integrated assessments, *Clim. Dyn.*, *14*, 291–303.
- Sokolov, A. P., C. E. Forest, and P. H. Stone (2003), Comparing oceanic heat uptake in aogcm transient climate change experiments, *J. Clim.*, *16*, 1573–1582.
- Webster, M., et al. (2003), Uncertainty analysis of climate change and policy response, *Clim. Change*, *61*, 295–320.
- Wigley, T. M. L., and S. C. B. Raper (1990), Natural variability of the climate system and detection of the greenhouse effect, *Nature*, *344*, 324–327.

C. E. Forest, A. P. Sokolov, and P. H. Stone, Room E40-427 MIT, 77 Massachusetts Ave, Cambridge, MA 02139, USA. (ceforest@mit.edu)